# Transmission Channel Compensation in Self-Synchronizing Chaotic Systems

by

Alan Edward Freedman

Submitted to the Department of Electrical Engineering and Computer Science
in partial fulfillment of the requirements for the degrees of

Master of Engineering in Electrical Engineering and Computer Science

and

Bachelor of Science in Electrical Science and Engineering

at the

MASSACHUSETTS INSTITUTE OF TECHNOLOGY

June 1995



Author ................................................................
Department of Electrical Engineering and Computer Science
May 26, 1995

Certified by ................................................................
Alan V. Oppenheim
Distinguished Professor of Electrical Engineering
Thesis Supervisor

Accepted by ................................................................
Frederic R. Morgenthaler
Chairman, Departmental Committee on Graduate Students

# Transmission Channel Compensation in Self-Synchronizing Chaotic Systems

by

Alan Edward Freedman

Submitted to the Department of Electrical Engineering and Computer Science
on May 26, 1995, in partial fulfillment of the
requirements for the degrees of
Master of Engineering in Electrical Engineering and Computer Science
and
Bachelor of Science in Electrical Science and Engineering

## Abstract

Certain classes of chaotic systems possess the property of self-synchronization, which allows two identical systems to synchronize when the second is driven by the first. Practical utilization of self-synchronizing chaotic systems depends upon their ability to withstand perturbations caused by imperfect communication channels. In this thesis the behavior of self-synchronizing chaotic systems under such circumstances is characterized, and compensation strategies are proposed.

We develop methods for recovering a transmitted signal produced by a self-synchronizing chaotic system and corrupted by an unknown, possibly time-varying, gain present in the transmission channel. We also explore effects of channel filtering and techniques for compensation. Strategies are presented to design compensating systems, ideally the inverse of the corrupting influences, which may be applied at the receiver.

Thesis Supervisor: Alan V. Oppenheim
Title: Distinguished Professor of Electrical Engineering

# Acknowledgments

I would like to acknowledge the contributions of the following individuals who have greatly assisted me in the completion of this thesis:

Professor Alan V. Oppenheim, who has consistently steered me toward productive research directions and offered both encouragement and constructive criticism to motivate my work;

Dr. Kevin Cuomo, who has answered question after question about the subtleties underlying his own research in this area, allowing me to gain more insight into issues relevant to my own research; and additionally, who has been willing to offer last-minute suggestions to aid in the completion of this document;

Paul Fiore and Richard Barron, whose interest and curiosity in my work kept me on my toes and provided me with opportunities to discuss my progress with my colleagues;

and Therese Honda, who has been patient, understanding, and always willing to offer her services as proofreader, brainstormer, or chef.

Thanks to each of you for providing me with the drive and the resources to successfully complete this project. I appreciate the efforts that all of you have made on my behalf.

# Contents

# List of Figures

# Chapter 1

# Introduction

Techniques have been developed recently for analyzing and synthesizing a particular class of nonlinear systems known as *self-synchronizing chaotic systems* [2]. Practical utilization of self-synchronizing chaotic systems depends in part on the systems' ability to withstand perturbations due to imperfect communication channels. In this thesis we characterize the behavior of self-synchronizing chaotic systems under such circumstances, and propose strategies for compensation.

Much interest in self-synchronizing chaotic systems stems from the potential use of chaotic signals as modulating signals for spread-spectrum communication systems. *Spread-spectrum communication systems*, which modulate the energy of an information-bearing signal over a large portion of the spectrum, recover the information by "cross-correlation of the received wide-band signal with a synchronously generated replica of the wide-band carrier" [1]. An advantage of using spread-spectrum techniques is that multiple independent carriers can share the same bandwidth and not interfere, increasing the communication capacity of the spectrum. This advantage can potentially be enhanced by using chaotic carrier signals, which have similar spectral characteristics to noise and may deceive an independent listener into assuming that no transmission is occurring when in fact one is. The appeal of spread-spectrum communications motivates an analysis of the properties of self-synchronizing chaotic systems.

A diagram of a chaotic spread-spectrum system is shown in Figure 1-1 [4]. The self-synchronizing chaotic system provides the backbone for the modulation and demodulation. The drive link between the chaotic drive and response systems is essential to the successful operation of the spread-spectrum system as a whole. We will focus solely on this link.

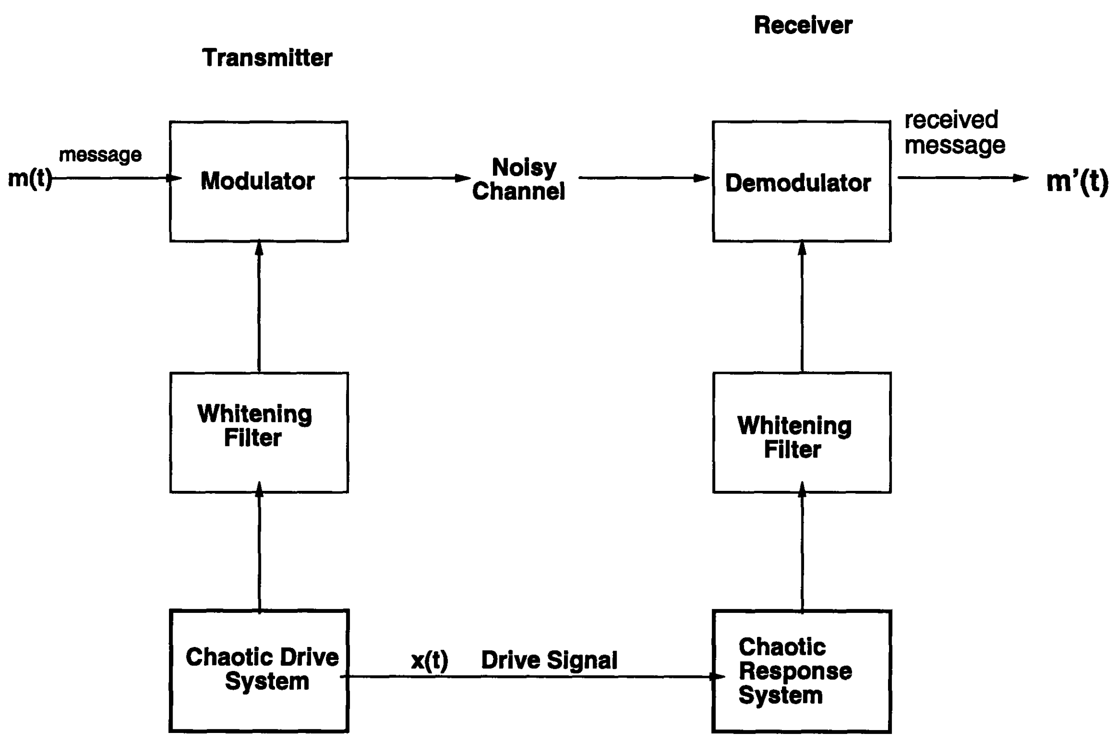


Figure 1-1: Chaotic Spread Spectrum System

The phenomenon of synchronization has been well-known for over fifty years and motivated much research in spread-spectrum communication during World War II [1]. Work in *chaotic* systems, however, is much more recent, only occurring within the past ten to fifteen years. The two topics were linked only five years ago, in 1990, when it was discovered that the self-synchronization property could exist within a chaotic system [6]. Since then, chaotic spread-spectrum systems have been analyzed, simulated [4], designed, implemented and tested [3], with excellent correspondence reported between theoretical and experimental results.

The basis for much of the research described in this thesis was a recent study which described general techniques for the analysis and synthesis of self-synchronizing chaotic systems [2]. The effects of additive noise on the quality of synchronization were investigated and documented. An issue which was not fully addressed was whether self-synchronizing chaotic systems can achieve approximate synchronization between transmitter and receiver in the presence of other variations in transmission channel characteristics. We will examine how effectively self-synchronizing chaotic systems can achieve approximate synchronization in the presence of gain or filtering in the transmission channel, and explore compensation techniques for recovering the original transmissions.

Since channel gain is, in some sense, the simplest form of channel disturbance, our investigation will begin with an analysis of gain effects on the quality of synchronization. Two techniques for gain compensation were considered: minimization of synchronization error, and comparison of average power in the received signal with theoretical results. The second converges quickly to a rough estimate of the compensating gain, but the first can determine the correct compensating gain with a higher degree of precision. If the gain is static, either technique will yield excellent results. On the other hand, a time-varying channel gain which varies slowly may require both constant tracking with a power comparison as well as tuning to eliminate the remaining error. The minimum interval over which power estimates can be computed, such that the variance of the set of estimates is within a user-specified tolerance, places an upper bound on the time variation of the gain.

A second topic which was investigated was channel filtering. The focus for solving the filtering problem was on infinite impulse-response (IIR) filters with finite impulse-response (FIR) inverse filters. An optimal FIR compensator can be realized by determining the set of filter coefficients which provide the best least-square-error fit to the inverse spectrum of the transmission channel. Alternatively, minimization of synchronization error is applicable in theory, but may be cumbersome in practice.

## 1.1 Outline of the Thesis

Chapter 2 defines the Lorenz transmitter-receiver system, explores the concept and properties of synchronization, and provides an explanation of the analysis procedure for experiments with the system. In this chapter definitions are developed which will be used throughout the thesis.

Chapter 3 examines the effects of channel corruption on the quality of synchronization providing a basis for compensation techniques. The chaos-to-error ratio (CER) is plotted as a function of channel parameters.

Chapter 4 introduces two strategies for gain compensation: (1) comparison of average power, and (2) minimization of synchronization error. The performance of each of these compensation techniques is analyzed.

Chapter 5 introduces two analogous strategies for filter compensation: (1) spectral comparison, and (2) (multi-dimensional) minimization of synchronization error. The performance of each of these compensation techniques is analyzed as well.

Chapter 6 summarizes the key results of this thesis and offers suggestions for further work on this topic.

# Chapter 2

# Self-Synchronization and the Lorenz System

*Chaotic* systems exhibit a *sensitive dependence on initial conditions*, meaning states which are nearly identical may not evolve similarly. The interconnection of two chaotic systems might be expected to mirror the locally unstable behavior of a single system. Under a certain set of conditions, however, synchronization of the interconnected systems can be observed.

*Synchronization* of a pair of systems is a coupling of the state variables in system S1 with the state variables in S2 such that S2's state is completely determined by S1's. A self-synchronizing system, then, has the following characteristic: if two copies of the system are produced, and a state variable from the *transmitting* system S1 drives the *receiving* system S2 in an appropriate manner, the state of the receiver will approach the state of the transmitter after a transient. Chaotic systems possessing the self-synchronization property, however, utilize a stable subsystem to achieve synchronization, *independent* of the initial conditions present [2].

Of the many chaotic systems which possess the self-synchronization property, the Lorenz transmitter-receiver system was chosen to be the prototype for this study. Current research in chaotic systems indicates that many of the qualitative properties of the Lorenz system can be observed in other chaotic systems as well. Within the Lorenz framework, the transmitter and receiver equations are

$$
\begin{aligned}
\dot{x} &= \sigma(y - x) \\
\dot{y} &= rx - y - xz \\
\dot{z} &= xy - bz
\end{aligned}
$$

$$
\begin{aligned}
\dot{x_r} &= \sigma(y_r - x_r) \\
\dot{y_r} &= rs(t) - y_r - s(t)z_r \\
\dot{z_r} &= s(t)y_r - bz_r.
\end{aligned}
$$

$$
\begin{aligned}
\text{where } s(t) &= \text{drive signal in the receiver equations} \\
x, y, z &= \text{transmitter state variables} \\
x_r, y_r, z_r &= \text{receiver state variables}
\end{aligned}
$$

The fact that these equations may lead to synchronization of the transmitter and receiver follows by considering the differences between the state variables of the transmitter and receiver:

$$[E_x \ E_y \ E_z] = [x \ y \ z] - [x_r \ y_r \ z_r]$$

The governing equations for these error signals are:

$$
\begin{aligned}
\dot{E}_x &= \sigma(E_y - E_x) \\
\dot{E}_y &= -E_y - s(t)E_z \\
\dot{E}_z &= s(t)E_y - bE_z.
\end{aligned}
$$

Now suppose that $s(t) = x(t)$; i.e., the receiving system is driven by one of the state variables of the transmitter. For the corresponding set of dynamic equations, it can be shown that $[E_x \ E_y \ E_z] = [0 \ 0 \ 0]$ is a globally stable fixed point [2]. In other words, the error between the transmitter and receiver state variables approaches zero as time evolves, or equivalently the transmitter and receiver must synchronize.

At $t = 0$, the state of the transmitting and receiving systems is summarized by a set of initial conditions $[x \;\; y \;\; z]_{init}$ and $[x_r \;\; y_r \;\; z_r]_{init}$. The state variables of the receiver synchronize to those of the transmitter by approximately $t = 2$. Synchronization is illustrated in Figure 2-1.

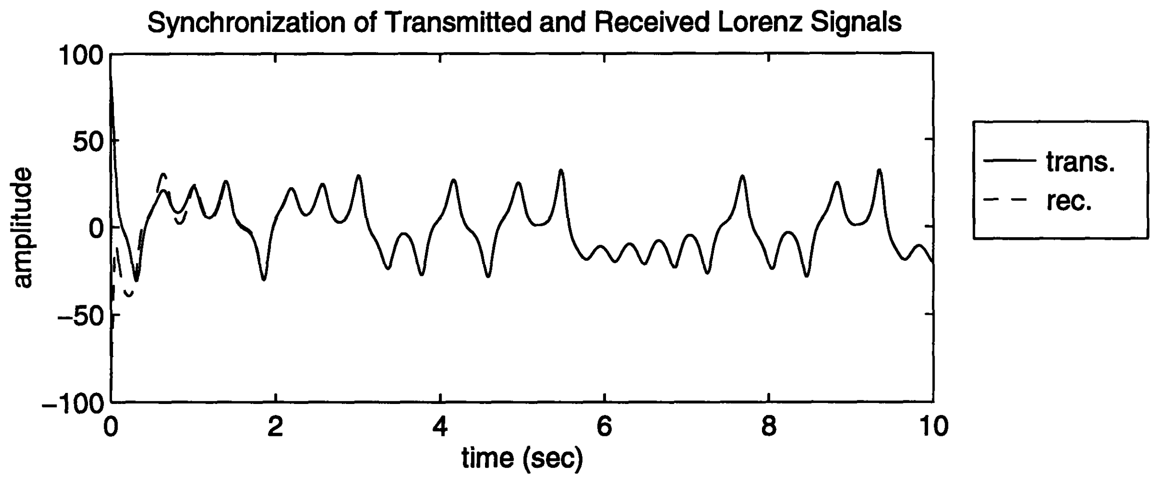


Figure 2-1: Synchronization

## 2.1 Spectrum of a Lorenz Signal

Though two Lorenz signals may synchronize with one another, the behavior of a single Lorenz signal as a function of time is highly dependent upon the initial conditions of the system which produces it. It is more natural to think of the set of signals which can be produced by the Lorenz system as sample paths of a random process. This model is not strictly accurate, since the dynamics of the system are deterministic, but allows the application of techniques which are used to analyze the behavior of random processes. Specifically, it is plausible to calculate the spectrum of a Lorenz signal based on the *statistical* properties of the class of Lorenz signals to which it belongs.

One means of obtaining an estimate for the power spectral density of a Lorenz signal is by calculating an *averaged periodogram.* This technique, normally applicable to stationary random signals, works well for the (pseudorandom) Lorenz signal since the dynamics of the Lorenz system are time-invariant. The averaged periodogram estimates the power in the signal at each frequency based on a truncated version of the signal.

The averaging of consecutive spectral estimates based on consecutive but non-overlapping sections of the original signal provides an asymptotically efficient estimate of the power in the signal. The estimate may be further smoothed by using non-rectangular windows ("modified periodogram") and/or averaging filters.

The spectrum of the Lorenz signal was calculated using a modified averaged periodogram. The modified averaged periodogram estimate of the Lorenz spectrum in Figure 2-1 was obtained using 100 5-second sections of a Lorenz signal, each windowed by the Hanning window. The relevant calculations can be found in Appendix A. Figure 2-2 shows the estimated spectrum of the transmitted signal $x(t)$ versus $t$ (in seconds). This and subsequent plots will assume that the variable $t$ in the Lorenz equations is measured in seconds. By selecting the time variable in the Lorenz equations to represent a different time unit, the time axis can be rescaled in an arbitrary fashion, placing the Lorenz signal in any specified frequency range.

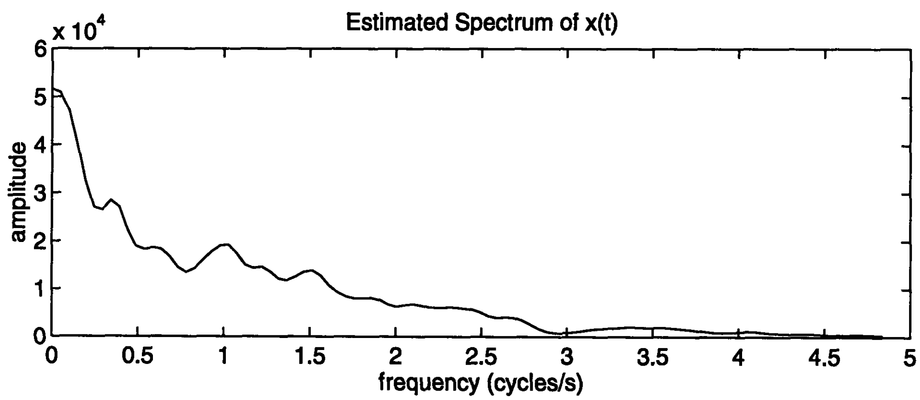


Figure 2-2: Estimated Spectrum of a Lorenz Signal

## 2.2 Analysis Procedure

### 2.2.1 Integration Algorithm

The Lorenz equations were numerically integrated using a fourth-order Runge-Kutta algorithm with a timestep of 0.0025. This value was chosen to ensure numerical stability. Appendix B contains the integration routines.

While setting up the numerical integration, we might assume that since $s(t)$ is created by transmitting $x(t)$ over a channel, we could include the analytic expression for $s(t)$ (in terms of $x(t)$) in the integration algorithm. We do not do this for the following reason. Suppose the drive signal $s(t)$ is represented as a vector of samples $s[n]$. with a spacing of $\delta$ seconds between samples. This vector contains all of the information available to the receiving party about the signal $x(t)$. However, noise perturbations present in the transmission channel in addition to the gain or filtering may result in an $s[n]$ which bears little resemblance to $x(t)$. Fourth-order Runge-Kutta integration computes, for example, $x(\delta)$ from $x(0)$ by averaging contributions from $x(\delta/2)$ among other quantities. This is possible for $x$ since it is defined on a continuous variable $t$, but not for $s[n]$. Since $s(\delta/2)$ is not available, we treat $s[n]$ as a vector of time-varying coefficients, rather than relating $s[n]$ analytically to $x(t)$.

Under ideal conditions (no noise), however, the quality of synchronization can be improved by modifying the Runge-Kutta formulation; specifically, interpolation of the drive signal decreases the energy in the synchronization error when no other perturbations are present. Nevertheless, in the interest of preserving the validity of the results obtained in this study under the most general set of circumstances, we shall treat $s(t)$ as described in the previous paragraph.

### 2.2.2 Parameter Values

At an early stage of these investigations, an array of tests was performed to examine the effects of parameter variations on several system properties. Specifically, $\sigma$ was varied from 8 to 16, $r$ from 40 to 70, and $b$ from 2 to 5. No significant qualitative differences were observed in the system behavior, suggesting that characterization of the Lorenz transmitter-receiver system at one set of parameter values was sufficient to understand the system dynamics. The values of the Lorenz parameters chosen for this study are $\sigma = 16,\ r = 60,\ b = 4$.

## 2.3 Quantities of Interest

Relevant system parameters include:

$$
\begin{aligned}
\tilde{x}(t) &= \text{received signal before compensation} \\
\tilde{x}(t) &= \text{received signal after compensation} \\
&= \text{signal which drives the receiving system} \\
e_x(t) &= s(t) - x_r(t) \\
&= \text{synchronization error} \\
&= \text{difference between received and reconstructed } x(t) \\
\bar{P}_x(t) &= \text{average power in } x(t) \\
\text{CER} &= \bar{P}_x(t)/\bar{P}_{e_x}(t) \\
&= \text{chaos-to-error ratio} \\
&= \text{quality of synchronization rating}
\end{aligned}
$$

Many measures were available to rate system performance: the average power in the synchronization error, length of time necessary for transient decay, several different signal-to-error ratios, among others. The measure which most effectively indicated compensation strategies was the chaos-to-error ratio (CER) defined above: the ratio of the average power in the transmitted signal $x(t)$ to the average power in the synchronization error $e_x(t)$. As we will see in the next chapter, the CER is a smooth function of channel gain, reaching its peak when the synchronization error is minimized, thus making it a natural choice for rating the quality of synchronization.

# Chapter 3

# Channel Corruption Effects

The problem facing the transmitting and receiving parties in a spread-spectrum communications system is ensuring the functionality of the link between the chaotic drive and response subsystems. Since the transmitter is generally unable to control the characteristics of the communications channel over which the chaotic signal is transmitted, the receiver's task is to compensate for the channel as well as possible. The following diagram illustrates how such a system might be implemented:

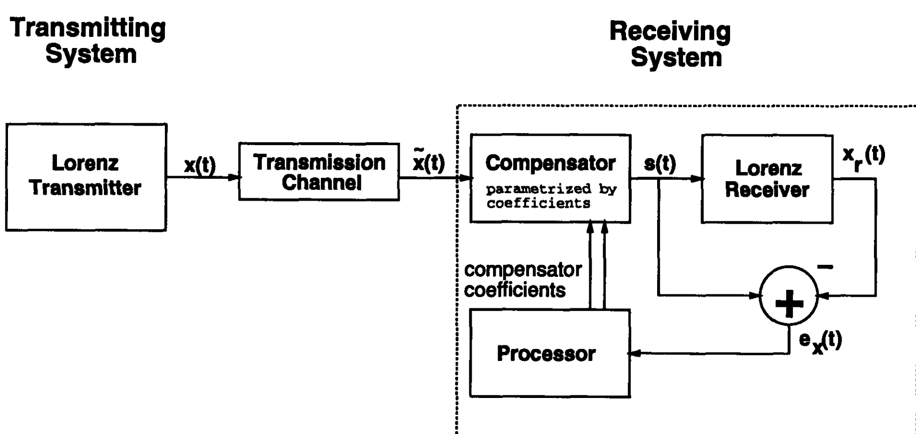


Figure 3-1: Chaotic Drive-Response Link with Channel Compensation

In general, the impulse response of the transmission channel is unknown, so a model must be assumed by the receiving party. For simplicity, suppose that the transmission channel imposes a time-varying gain $G(t)$ on the intended drive signal $x(t)$, resulting in the uncompensated received signal $\tilde{x}(t) = G(t)x(t)$. If $G(t) = 1$ for all $t$, and the compensator's output is given by $s(t) = \tilde{x}(t)$, then $s(t) = x(t)$ and any difference between the initial conditions in the transmitter and those in the receiver will decay in a transient fashion. Thus, synchronization will result, as described earlier. If the transmission channel gain is not unity, and there is no compensation, the synchronization error incurred becomes significant; i.e., as the gain varies in either direction away from $G = 1$, synchronization quality decreases.

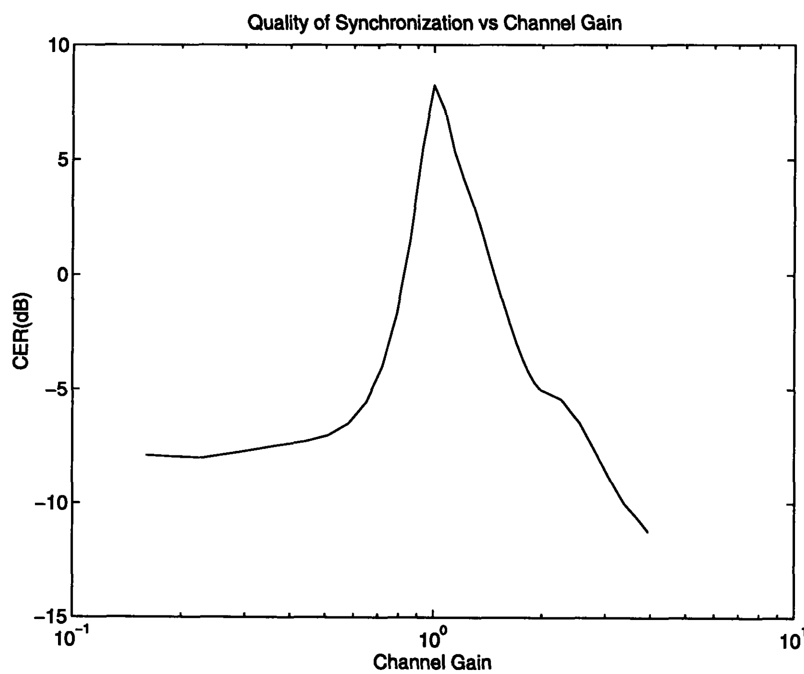


Figure 3-2: Quality of Synchronization versus Channel Gain

Figure 3-2 shows the CER (in decibels) plotted versus channel gain, over several octaves of variation in channel gain. The key feature of this curve is its unimodality; it contains a global maximum at $G = 1$. For gains which are greater than unity, the energy in the synchronization error approaches the energy of the received signal, which is proportional to $G^2$. Since $\bar{P}_x$ is independent of G, the CER falls off approximately as $1/G^2$. For gains much smaller than unity, the average magnitude of the reconstructed signal is greater, surprisingly, than the average magnitude of $x(t)$. Again, the CER falls off with decreasing gain.

A slightly more complicated model might represent the channel transfer function as a one-pole discrete-time filter:

$$
\begin{aligned}
H(z) &= \frac{u}{1 - vz^{-1}} \\
\text{where } u, v &= \text{filter parameters}
\end{aligned}
$$

Using this model for the channel filter, Figure 3-3 (a) plots filter magnitude versus radian frequency with $u = 1$ and $v = 0.1$.

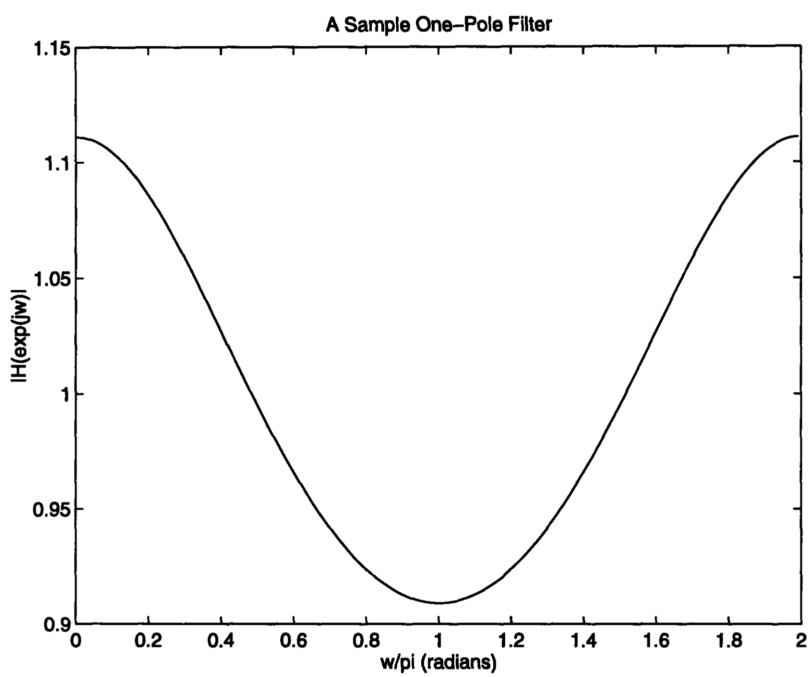


Figure 3-3: A Sample One-Pole Filter

We would like to scale the filter spectrum so that one period of the filter spectrum approximately overlaps the Lorenz spectrum. Suppose we upsample the one-pole filter by a factor $N$. This has the effect of compressing the filter spectrum by the same factor $N$. The expression which represents the newly created all-pole filter is

$$
\begin{aligned}
H(z) &= \frac{u}{1 - vz^{-N}} \\
\text{where } N &= \text{upsampling factor}
\end{aligned}
$$

The corresponding continuous-time transfer function is found by letting $z = e^{sT}$ in the above expression, where $s$ represents continuous-time frequency in radians/second. We then have:

$$
H(s) = \frac{u}{1 - ve^{-sNT}}
$$

Using this filter model, it is possible to examine the CER as a function of both $u$ and $v$, with N = 100. This three-dimensional surface, illustrated in Figure 3-4 peaks in a similar fashion to the two-dimensional plot of CER vs gain. If one parameter is held constant while the other is varied, a cross-section of the 3-D plot is generated. Note that this surface is unimodal; that is, the global maximum at $u = 1, v = 0$ is the only extreme point on the surface. The cross-sectional plots also indicate that each cross-section is unimodal. Unfortunately, the peaks do not coincide; $u = 1$ is not necessarily the cross-sectional peak for all values of $v$, and similarly $v = 0$ is not necessarily the peak at all values of $u$. This fact will hinder attempts at compensation, as we will see in Chapter 5.

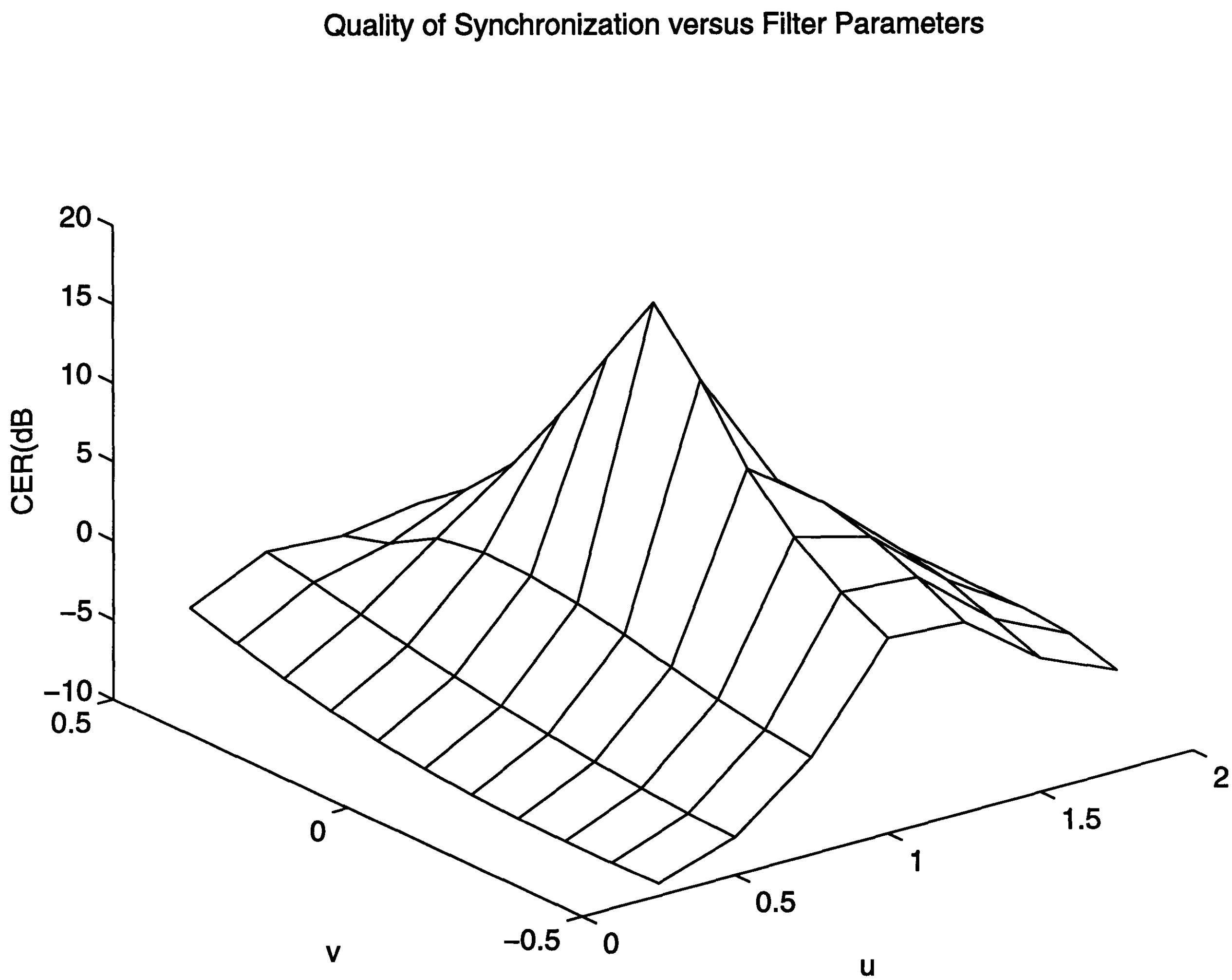


Figure 3-4: Quality of Synchronization versus Filter Parameters

# Chapter 4

# Gain Compensation Strategies

## 4.1 Real-Time Coarse Adjustment by Comparison of Average Power

We have seen that unless the transmission channel gain is unity, the transmitter will not synchronize with the receiver. Assuming the channel imparts only a gain to the transmitted signal, the ideal compensator is a gain block with gain $C(t) = G^{-1}(t)$.

At the receiver, $\tilde{x}(t) = G(t)x(t)$ is readily obtainable. Since the receiver is subject to different initial conditions than the transmitter, $x(t)$ itself is not available at the receiver. Note, however, that the receiver, being identical to the transmitter in all other respects, is capable of generating another sample path of the random process, with the same statistical properties. It is therefore possible for the receiver to compute $\bar{P}_x$ off-line. This observation motivates a strategy for making a rough estimate of the transmission channel gain $G(t)$.

An estimator of $C(t)$ may be obtained by first computing an approximate value for $\bar{P}_{\tilde{x}}(t)$, the average power in the received signal at time $t$. Let $t_{min}$ be the minimum time interval required to calculate a stable estimate of $\bar{P}_{\tilde{x}}(t)$. Then the following strategy gives an estimate $\hat{C}$ of the compensating gain $C$, as a function of time:

**STRATEGY G1:**

- Over the time interval $(t - t_{min}, t)$, compute $\bar{P}_{\tilde{x}}(t)$.
- $\hat{C}(t) = \sqrt{\bar{P}_x/\bar{P}_{\tilde{x}}}$

Given the earlier discussion of Lorenz spectrum estimation, we would like to know the interval length (in seconds) needed to compute a valid estimate of the power in a chaotic signal. The answer to this question may be found by examining the variance of Lorenz power estimates as a function of interval length. This relationship is plotted in Figure 4-1.

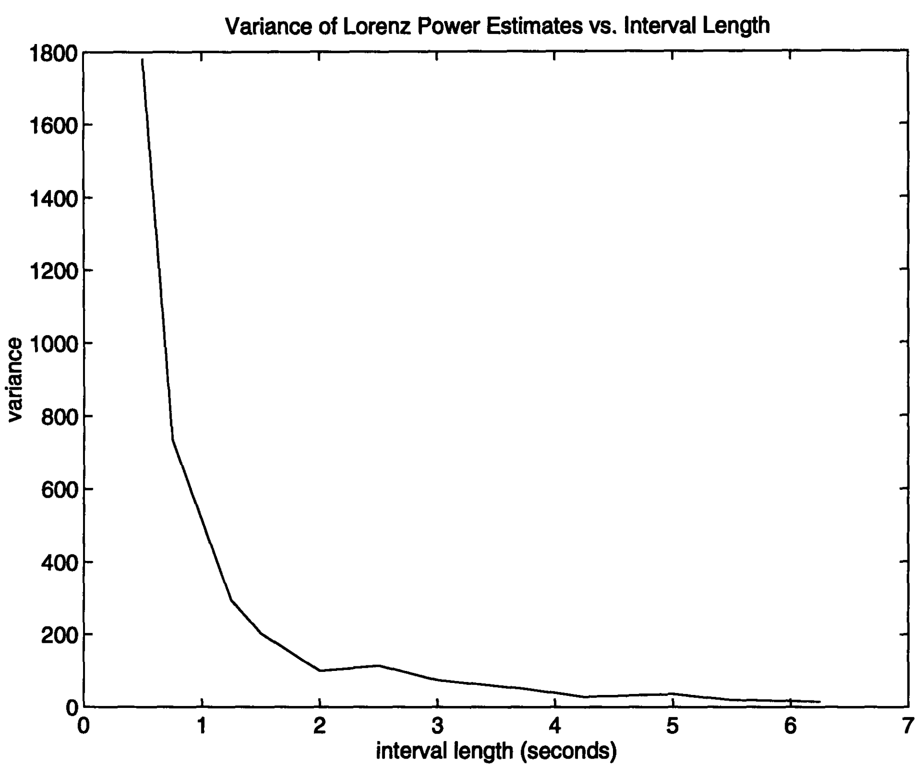


Figure 4-1: Stability of Power Estimates

As illustrated, the variance of the estimate of $\bar{P}_x$ levels off at $t_{min} \approx 2$ seconds. Assuming that we choose an interval of length at least $t_{min}$ over which to compute the power, we can be reasonably assured that the estimate is accurate.

Given $t_{min}$, we can quantify the maximum rate at which $G(t)$ must vary for real-time gain compensation to be feasible. If $G(t)$ varies slowly enough so that the gain is approximately constant on time intervals of length $t_{min}$, the above technique will yield an excellent estimate of $C(t)$. A good rule of thumb is that the spectrum of $G(t)$ should be bandlimited to approximately $2\pi/(10 \cdot t_{min})$.

Figure 4-2 shows a sample $G(t) = 0.7 + 0.5\ \sin(2\pi(0.2)t)$ and the corresponding $\hat{C}(t)$.

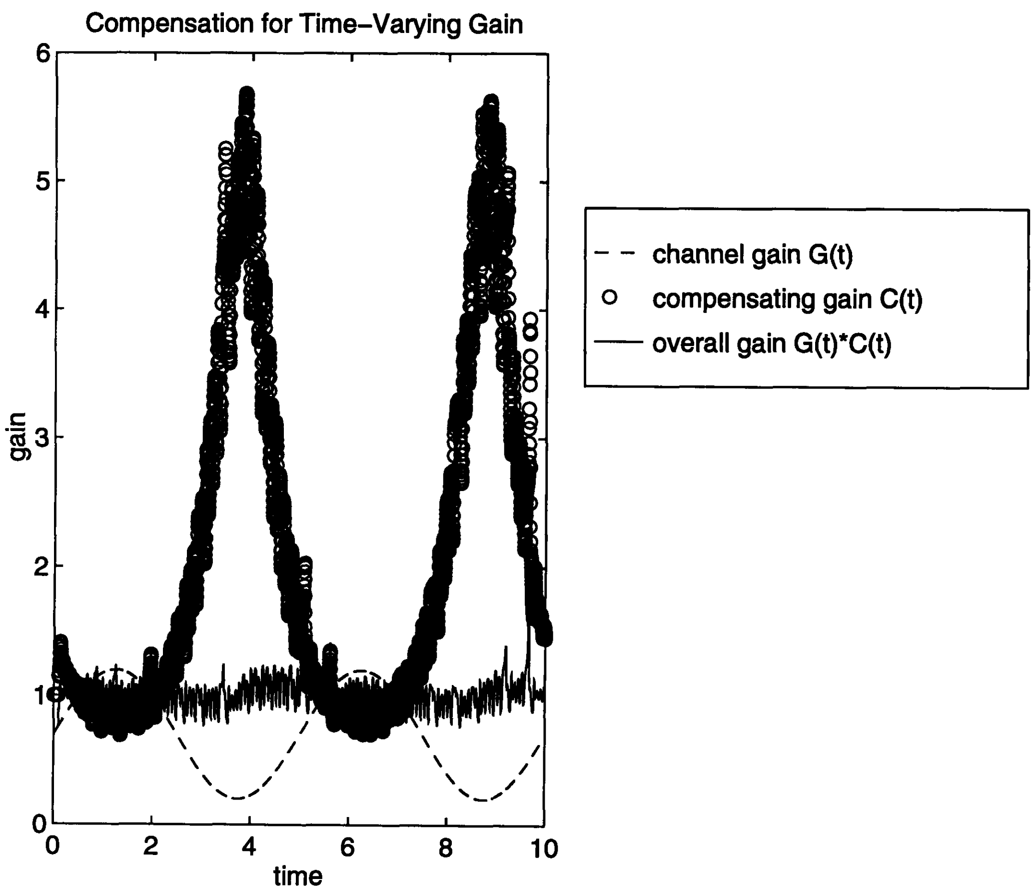


Figure 4-2: Compensation for Time-Varying Gain

## 4.2 Fine Adjustment by Analysis of Chaos-to-Error Ratio

If the gain is static, a more effective strategy may be implemented. Let $G(t) = G$, for all $t$. Over a wide range of channel gains, the $CER$-vs-gain characteristic has a single local extremum, which is its global maximum. Because the gain is not time-varying, it is possible to calculate the $CER$ at several values of $C$ to pinpoint the location of the maximum. The following method may be employed to determine the true value of $C$:

**STRATEGY G2:**

- Set $C = 1$, and calculate the $CER$ from $\bar{P}_x(t)$ (known) and $\bar{P}_{e_x}(t)$ (varies as a function of $G$).

- Vary the value of $C$ slightly away from 1 and recalculate $CER_x$.

- If the new value of $CER_x$ is greater than the old value, continue to vary $C$ in the same direction. If the new value is smaller than the old value, vary $C$ in the opposite direction. Continue in this manner until $CER_x$ ceases to increase. The value of $C$ at which this occurs is the correct compensating gain.

The system characteristics which we exploit in employing this strategy are (1) the unimodality of the $CER$-vs-gain curve and (2) the stationary channel gain. The first property permits gradient search; that is, iterating toward the peak of the curve by examining its slope. The second allows an initial guess of the correct compensating gain to be refined until it is as close to optimal as possible.

A combination of the two proposed methods can monitor a very slowly varying channel gain. For example, we might achieve a rough estimate of $C$ by comparing average powers, and then performing fine-adjustment in the remaining time until the channel gain variation is significant enough to force a new rough estimate to be made.

# Chapter 5

# Filter Compensation Strategies

## 5.1 Real-Time Coarse Adjustment by Spectral Comparison

The more general channel compensation problem is the deconvolution of the (unknown) transfer function of the transmission channel. Theoretically, the correct compensating filter could be precisely determined using a method analogous to the *comparison of average power* strategy G1. An estimator, $\hat{C}(s)$, could be obtained by computing an approximation to $S_{\tilde{x}\tilde{x}}(s)$, the power spectral density of the received signal. We would then have:

$$|\hat{C}(s)| = \sqrt{S_{xx}(s)/S_{\tilde{x}\tilde{x}}(s)}$$

In practice, however, there is a problem with this approach. Estimation of the spectrum of a signal using averaged periodograms is only asymptotically efficient, requiring a large amount of data before the variance of the spectral estimate decreases to within some specified tolerance. Real-time estimation of the unknown, possibly time-varying channel filter, is made much more tractable by assuming a model for the type of filtering present. Given the model and a set of experimental data, a best-fit analysis on the data can determine the most likely model parameters. In the context of channel compensation, the equivalent goal is to specify the parameters of the optimal compensating filter which must be applied to the received signal in order to recover the original transmission.

Recall the all-pole channel filter of the form:

$$H(s) \;=\; u/(1 - ve^{-sNT}),$$

The corresponding compensator, an all-zero filter, has frequency response $C(s) = H^{-1}(s)$, and may be represented as an FIR filter of length $(N+1)$:

$$\hat{C}(s) = \hat{a} - \hat{b}e^{-sNT}$$

Note, however, $(N-1)$ of these coefficients are zero; only the first and last coefficients are nonzero. The theoretical values of $a$ and $b$ in terms of $u$ and $v$ are $a = u^{-1}, b = vu^{-1}$. We will apply essentially the same strategies to estimate the compensator coefficients as were applied to the gain problem; the presence of additional degrees of freedom (multiple coefficients to select as opposed to only one) only causes slight modifications to the original compensation strategies. Also, although $u, v, a,$ and $b$ may themselves be nonstationary, we choose to suppress the time parameter in our filter expressions. Clearly, the limitations on compensation which apply to time-varying gains similarly apply to time-varying filter coefficients.

The first strategy we will consider for estimation of the filter coefficients $a$ and $b$ will be the *comparison of power spectra* technique. By definition, the following relationships are true for the actual power spectral densities:

$$S_{\tilde{x}\tilde{x}}(s) \;=\; H(s)H(-s)S_{xx}(s) \tag{5.1}$$

$$S_{\tilde{x}\tilde{x}}(jw) = |H(jw)|^2 S_{xx}(jw) \tag{5.2}$$

The following strategy, then, estimates the two coefficients $a$ and $b$ which comprise $\hat{C}(s) = \hat{a} - \hat{b}e^{-sNT}$:

**STRATEGY F1:**

- Compute a spectral estimate $\hat{S}_{\tilde{x}\tilde{x}}(j\omega_k)$ for the spectrum of the received signal.
- $|\hat{C}(j\omega_k)| = \sqrt{S_{xx}(j\omega_k)/\hat{S}_{\tilde{x}\tilde{x}}(j\omega_k)}$
- To locate the coefficients $\hat{a}$ and $\hat{b}$, use a least-square-error optimization routine to find the best-fit solution to the following set of k equations (choose k as large as is feasible given computing constraints, choose the set of frequencies $\omega_k$ to sample one period of the filter frequency response)

$$\hat{C}(j\omega_k) = \hat{a} - \hat{b}e^{\omega_k NT} \tag{5.3}$$

Figure 5-1 illustrates this compensation strategy. The recovered filter spectrum, shown in the second plot, is an approximation to the actual filter spectrum shown in the first plot. To estimate the coefficients of the all-pole filter which this spectrum is supposed to represent, the above equations were evaluated at five frequencies equally spaced over one period of the spectrum, drawn in as x's on the second plot. Within a few percent, the filter coefficients were recovered, from which it was possible to approximately determine an approriate compensating filter.

## 5.2 Fine Adjustment by Analysis of Chaos-to-Error Ratio

The second strategy we will consider will be the technique based on *minimization of synchronization error.* As we have seen earlier, the CER (as a function of the transmission channel filter coefficients $u$ and $v$) is unimodal over a wide range surrounding the peak at the optimal $(u, v) = (1, 0)$, at which synchronization occurs. Recall that

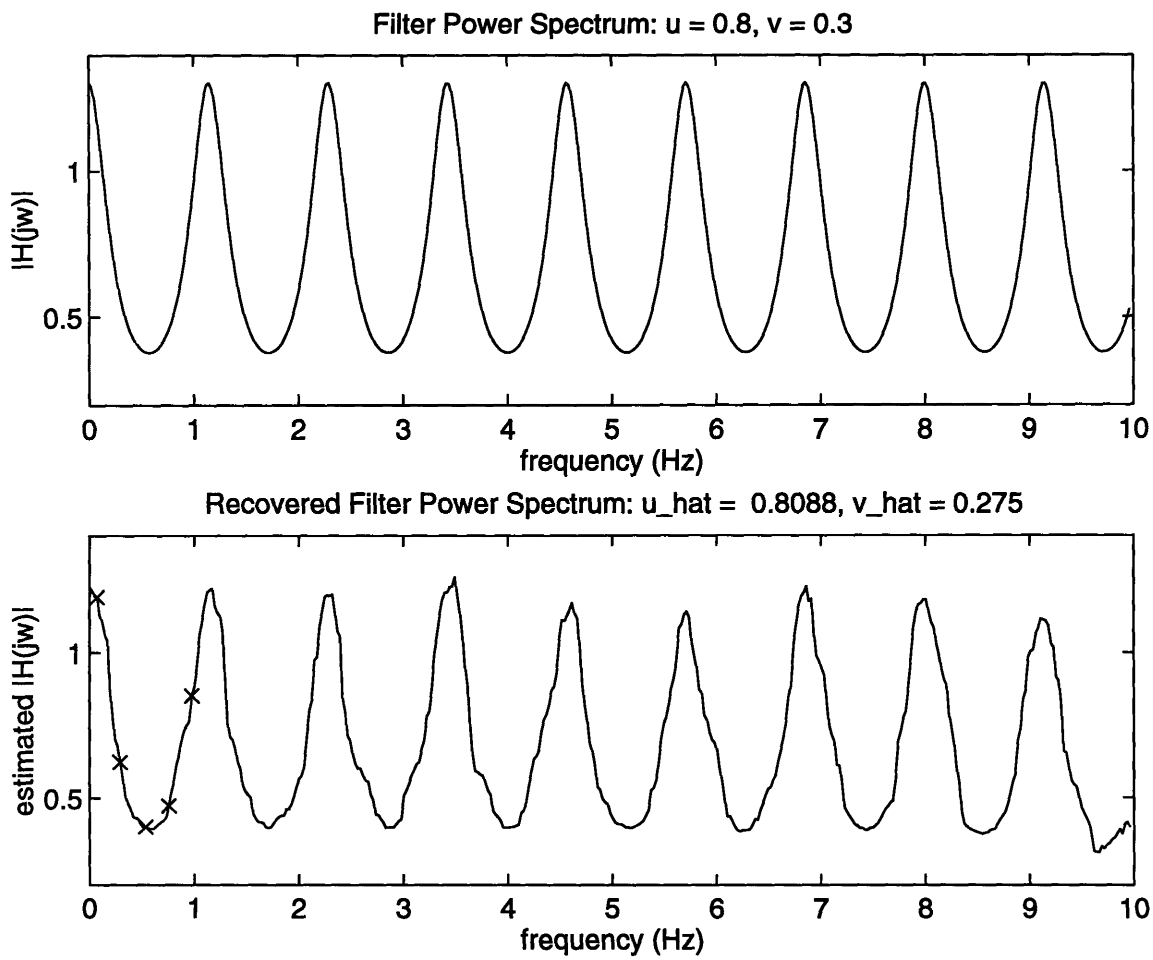


Figure 5-1: Comparison of Original and Estimated Channel Filter Spectra

$u = 1$ is not the cross-sectional peak for all values of $v$, and similarly $v = 0$ is not the peak at all values of $u$. Therefore, it is not valid to first maximize the CER over one of the variables, then maximize the remaining function of the other variable, in order to locate the global maximum.

What is possible to implement, however, is a multi-dimensional gradient search subroutine. Such an algorithm computes the direction of maximum (positive) variation in the CER at a particular point $(u_0,\ v_0)$. This lends itself to the following strategy, analogous to gain strategy G2:

**STRATEGY F2:**

- Set $a = 1, b = 0$, and calculate the $CER$ from $\bar{P}_x(t)$ (known) and $\bar{P}_{e_x}(t)$ (varies as a function of $u$ and $v$).

- Compute the direction of maximum positive variation in the $CER$ at the current values of $a$ and $b$.

- Vary the values of $a$ and $b$ in the direction of increasing $CER$. Repeat the gradient search until the peak of the $CER$ surface is located. The values of $a$ and $b$ at which this occurs are the correct compensating coefficients.

The difficulty in implementing strategy F2 is in creating a real-time gradient-search routine. Again, this strategy is more appropriate for channel compensation which need not take place in real-time. As before, a combination of the above methods may be very well-suited to monitor very slowly varying channel characteristics.

# Chapter 6

# Conclusions

## 6.1 Summary of Key Results of this Thesis

We have examined the behavior of self-synchronizing chaotic systems which are subject to transmission channel corruption. The quality of synchronization is greatest when the transmission channel is unperturbed, and falls off uniformly when the channel contains gain or filtering effects. The unimodality of the CER-vs-gain curve provides a means of compensating for static channel gains, but comparison of average powers offers the ability for real-time compensation of time-varying channel gains. In the channel filtering case, spectral comparison is a much more viable means of compensation than multi-dimensional gradient search.

## 6.2 Suggestions for Further Work on this Topic

The many simplifying assumptions incorporated into this study point to avenues for further research concerning self-synchronizing chaotic systems. Attempts to observe similar behaviors to those exhibited by the Lorenz transmitter-receiver system within other chaotic frameworks would certainly be worthwhile.

The filter compensation problem has only been touched on; relevant issues which have not yet been explored include how well the spectrum of a chaotic signal can, in general, be estimated; if it were the case that the entire spectrum could be exactly computed, then the optimal compensator would be available in the form of the inverse filter. Existing techniques for computing spectral estimates are subject to computational constraints; a better approach might include a search for compensators which are nearly optimal and require only small amounts of computing resources to operate.

# Appendix A

# Calculations

Calculation of the periodogram of x[n]:

Let $x[n]$ be a discrete-time signal whose spectrum is to be estimated.

Let $w[n]$ be the window which captures a time-limited portion of $x[n]$, yielding $v[n] = w[n]x[n]$.

Let $L$ be the length of $w[n]$; $w[n]$ is nonzero on $[0, L-1]$.

Then $I(w)$, the periodogram estimate of $|X(e^{jw})|^2$, is given by:

$$V(e^{jw}) = \sum_{n=0}^{L-1} v[n]e^{-jwn} \tag{A.1}$$

$$I(w) = \frac{1}{LU}|V(e^{jw})|^2 \tag{A.2}$$

where $U$ is the normalizing constant

$$U = \frac{1}{L}\sum_{n=0}^{L-1}(w[n])^2 \tag{A.3}$$

Calculation of the an averaged periodogram of $x[n]$:

Let $K$ consecutive segments, each of length $L$, be chosen from $x[n]$. Denote these by $x_i[n], i = 1, 2, .., k$.

Let $w[n]$ be the window applied to each segment, yielding $v[n] = w[n]x_i[n]$.

Then $I(w)$, the periodogram estimate of $|X(e^{jw})|^2$, is given by:

$$V_i(e^{jw}) = \sum_{n=0}^{L-1} v_i[n]e^{-jwn} \tag{A.4}$$

$$I_i(w) = \frac{1}{LU}|V_i(e^{jw})|^2 \tag{A.5}$$

$$I(w) = \frac{1}{K}\sum_{i=1}^{K} I_i(w) \tag{A.6}$$

# Appendix B

# Source Code

The following Matlab scripts were made available by Dr. Kevin Cuomo for integration of the Lorenz equations.

```
function [x1,x2,x3] = lorcirc(tinc,tf,x0,sig,rr,b,T);
%  This Matlab script integrates the Lorenz transmitter equations from
%  0 to tf with time increment tinc.
%  x0 is the initial state of the transmitter.
%  sig, rr, b are the Lorenz parameters sigma, r, and b.
%  T adjusts the signal timescale.

numinc=ceil(tf/tinc);
x10=x0(1);
x20=x0(2);
x30=x0(3);
x1(1)=x10;
x2(1)=x20;
x3(1)=x30;
for i=1:numinc
   r=rr;
  a1=tinc*T*sig*(x20-x10);
  a2=tinc*T*(-x10*x30+r*x10-x20); a3=tinc*T*(x10*x20-b*x30);
  b1=tinc*T*sig*((x20+a2/2)-(x10+a1/2));
  b2=tinc*T*((x10+a1/2)*(x30+a3/2)+r*(x10+a1/2)-(x20+a2/2));
  b3=tinc*T*((x10+a1/2)*(x20+a2/2)-b*(x30+a3/2));
  c1=tinc*T*sig*((x20+b2/2)-(x10+b1/2));
  c2=tinc*T*((x10+b1/2)*(x30+b3/2)+r*(x10+b1/2)-(x20+b2/2));
  c3=tinc*T*((x10+b1/2)*(x20+b2/2)-b*(x30+b3/2));
```

```
  d1=tinc*T*sig*((x20+c2)-(x10+c1));
  d2=tinc*T*((x10+c1)*(x30+c3)+r*(x10+c1)-(x20+c2));
  d3=tinc*T*((x10+c1)*(x20+c2)-b*(x30+c3));

  x1(i+1)=x10+(a1+2.*b1+2.*c1+d1)/6.;
  x2(i+1)=x20+(a2+2.*b2+2.*c2+d2)/6.;
  x3(i+1)=x30+(a3+2.*b3+2.*c3+d3)/6.;
  x10=x1(i+1);
  x20=x2(i+1);
  x30=x3(i+1);
end
```

```
function [x1,x2,x3] = lorrecr(tinc,tf,x0,sig,rr,b,d,T);
%  This Matlab script integrates the Lorenz receiver equations from
%  0 to tf with time increment tinc.
%  x0 is the initial state of the receiver.
%  d is the drive signal $s(t)$.

numinc=ceil(tf/tinc);
x10=x0(1);
x20=x0(2);
x30=x0(3);
x1(1)=x10;
x2(1)=x20;
x3(1)=x30;
for i=1:numinc
  r=rr;
  a1=tinc*T*sig*(x20-x10);
  a2=tinc*T*(-d(i)*x30+r*d(i)-x20);
  a3=tinc*T*(d(i)*x20-b*x30);
  b1=tinc*T*sig*((x20+a2/2)-(x10+a1/2));
  b2=tinc*T*(-d(i)*(x30+a3/2)+r*d(i)-(x20+a2/2));
  b3=tinc*T*(d(i)*(x20+a2/2)-b*(x30+a3/2));
  c1=tinc*T*sig*((x20+b2/2)-(x10+b1/2));
  c2=tinc*T*(-d(i)*(x30+b3/2)+r*d(i)-(x20+b2/2));
  c3=tinc*T*(d(i)*(x20+b2/2)-b*(x30+b3/2));
  d1=tinc*T*sig*((x20+c2)-(x10+c1));
  d2=tinc*T*(-d(i)*(x30+c3)+r*d(i)-(x20+c2));
  d3=tinc*T*(d(i)*(x20+c2)-b*(x30+c3));

  x1(i+1)=x10+(a1+2.*b1+2.*c1+d1)/6.;
  x2(i+1)=x20+(a2+2.*b2+2.*c2+d2)/6.;
  x3(i+1)=x30+(a3+2.*b3+2.*c3+d3)/6.;
  x10=x1(i+1);
  x20=x2(i+1);
  x30=x3(i+1);
end
```

# Bibliography


[1] Charles E. Cook et al., editors. *Spread-Spectrum Communications.* IEEE Press, New York, NY, 1983.

[2] Kevin M. Cuomo. *Analysis and Synthesis of Self-Synchronizing Chaotic Systems.* PhD thesis, Massachusetts Institute of Technology, MIT Research Laboratory of Electronics, February 1994.

[3] Kevin M. Cuomo and Alan V. Oppenheim. *Synchronized Chaotic Circuits and Systems for Communications.* MIT Research Laboratory of Electronics, Technical Report No. 575, Massachusetts Institute of Technology, 1992.

[4] Kevin M. Cuomo, Alan V. Oppenheim, and Steven H. Isabelle. *Spread Spectrum Modulation and Signal Masking Using Synchronized Chaotic Systems.* MIT Research Laboratory of Electronics, Technical Report No. 570, Massachusetts Institute of Technology, 1992.

[5] Alan V. Oppenheim and Ronald W. Schafer. *Discrete-Time Signal Processing.* Prentice Hall, Englewood Cliffs, NJ, 1989.

[6] Pecora, L. M. and T. L. Carroll. "Synchronization in Chaotic Systems". *Physical Review Letters,* 64(8):821–824, February 1990.